NATIONAL ADVISORY COMMITTEE FOR AERONAUTICS

REPORT No. 869

ISOLATED AND CASCADE AIRFOILS WITH PRESCRIBED VELOCITY DISTRIBUTION

By ARTHUR W. GOLDSTEIN and MEYER JERISON

1947

For sale by the Superintendent of Documents, U. S. Government Printing Office, Washington 25, D. C. - - - - - - - - Price 15 cents

AERONAUTIC SYMBOLS

1. FUNDAMENTAL AND DERIVED UNITS

	Symbol	Metric		English	
		Unit	Abbreviation	Unit	Abbreviation
Length	l	meter	m	foot (or mile)	ft (or mi)
Time	t	second	s	second (or hour)	sec (or hr)
Force	F	weight of 1 kilogram	kg	weight of 1 pound	lb
Power	P	horsepower (metric)		horsepower	hp
Speed	V	kilometers per hour	kph	miles per hour	mph
		meters per second	mps	feet per second	fps

2. GENERAL SYMBOLS

W Weight$=mg$

g Standard acceleration of gravity$=9.80665$ m/s^2 or 32.1740 ft/sec^2

m Mass$=\frac{W}{g}$

I Moment of inertia$=mk^2$. (Indicate axis of radius of gyration k by proper subscript.)

μ Coefficient of viscosity

ν Kinematic viscosity

ρ Density (mass per unit volume)

Standard density of dry air, 0.12497 kg-m^{-4}-s^2 at 15° C and 760 mm; or 0.002378 lb-ft^{-4} sec^2

Specific weight of "standard" air, 1.2255 kg/m^3 or 0.07651 lb/cu ft

3. AERODYNAMIC SYMBOLS

S Area

S_w Area of wing

G Gap

b Span

c Chord

A Aspect ratio, $\frac{b^2}{S}$

V True air speed

q Dynamic pressure, $\frac{1}{2}\rho V^2$

L Lift, absolute coefficient $C_L=\frac{L}{qS}$

D Drag, absolute coefficient $C_D=\frac{D}{qS}$

D_0 Profile drag, absolute coefficient $C_{D_0}=\frac{D_0}{qS}$

D_i Induced drag, absolute coefficient $C_{D_i}=\frac{D_i}{qS}$

D_p Parasite drag, absolute coefficient $C_{D_p}=\frac{D_p}{qS}$

C Cross-wind force, absolute coefficient $C_C=\frac{C}{qS}$

i_w Angle of setting of wings (relative to thrust line)

i_t Angle of stabilizer setting (relative to thrust line)

Q Resultant moment

Ω Resultant angular velocity

R Reynolds number, $\rho\frac{Vl}{\mu}$ where l is a linear dimension (e.g., for an airfoil of 1.0 ft chord, 100 mph, standard pressure at 15° C, the corresponding Reynolds number is 935,400; or for an airfoil of 1.0 m chord, 100 mps, the corresponding Reynolds number is 6,865,000)

α Angle of attack

ϵ Angle of downwash

α_0 Angle of attack, infinite aspect ratio

α_i Angle of attack, induced

α_a Angle of attack, absolute (measured from zero-lift position)

γ Flight-path angle

ERRATA

NACA REPORT 869

ISOLATED AND CASCADE AIRFOILS WITH PRESCRIBED VELOCITY DISTRIBUTION

By Arthur W. Goldstein and Meyer Jerison

Page 13, Column 1: The left-hand side of equation (B7) should be $w'(z)$ instead of (z)

NACA-Langley - 10-11-49 - 1500

REPORT No. 869

ISOLATED AND CASCADE AIRFOILS WITH PRESCRIBED VELOCITY DISTRIBUTION

By ARTHUR W. GOLDSTEIN and MEYER JERISON

Flight Propulsion Research Laboratory
Cleveland, Ohio

National Advisory Committee for Aeronautics

Headquarters, 1724 F Street NW, Washington 25, D. C.

Created by act of Congress approved March 3, 1915, for the supervision and direction of the scientific study of the problems of flight (U. S. Code, title 49, sec. 241). Its membership was increased to 15 by act approved March 2, 1929. The members are appointed by the President, and serve as such without compensation.

TECHNICAL COMMITTEES

AERODYNAMICS
POWER PLANTS FOR AIRCRAFT
AIRCRAFT CONSTRUCTION
OPERATING PROBLEMS
SELF-PROPELLED GUIDED MISSILES
INDUSTRY CONSULTING

Coordination of Research Needs of Military and Civil Aviation
Preparation of Research Programs
Allocation of Problems
Prevention of Duplication
Consideration of Inventions

LANGLEY MEMORIAL AERONAUTICAL LABORATORY,
Langley Field, Va.

AMES AERONAUTICAL LABORATORY,
Moffett Field, Calif.

FLIGHT PROPULSION RESEARCH LABORATORY,
Cleveland Airport, Cleveland, Ohio

Conduct, under unified control, for all agencies, of scientific research on the fundamental problems of flight

OFFICE OF AERONAUTICAL INTELLIGENCE,
Washington, D. C.

Collection, classification, compilation, and dissemination of scientific and technical information on aeronautics

REPORT No. 869

ISOLATED AND CASCADE AIRFOILS WITH PRESCRIBED VELOCITY DISTRIBUTION

By Arthur W. Goldstein and Meyer Jerison

SUMMARY

An exact solution of the problem of designing an airfoil with a prescribed velocity distribution on the suction surface in a given uniform flow of an incompressible perfect fluid is obtained by replacing the boundary of the airfoil by vortices. By this device, a method of solution is developed that is applicable both to isolated airfoils and to airfoils in cascade. The conformal transformation of the designed airfoil into a circle can then be obtained and the velocity distribution at any angle of attack computed. Numerical illustrations of the method are given for the airfoil in cascade.

INTRODUCTION

The problem of increasing the output per stage in axial-flow compressors and turbines involves the use of high-solidity (closely spaced blades) stages of highly cambered blades. In addition, the velocity distribution must be carefully selected as a function of arc length along the airfoil (blade section) boundary in order to avoid flow separation or excessively high local velocities.

Several methods are available for obtaining an airfoil with a prescribed velocity distribution. The methods that lead to theoretically exact results are based on conformal-mapping theory. (See references 1 and 2.) In reference 3, Mutterperl extends the method of conformal mapping to solve the problem of computing a cascade of airfoils with prescribed velocity distribution but, for cascades with closely spaced or highly cambered airfoils, this procedure becomes very cumbersome. Approximate solutions have been obtained by placing singularities such as vortices, sources, and sinks in a uniform stream. The shape of sections of airfoils in cascade can also be computed by distributing such singularities periodically throughout the region of the cascade, as described by Ackeret (reference 4).

Because these vortex methods are not exact, a method with the vortices on the boundaries of the cascade airfoils was developed. This method gives a theoretically exact solution without the computation difficulties encountered in conformal-mapping methods for highly cambered airfoils or closely spaced cascades. Furthermore, for the same accuracy in computing the airfoil shape, this vortex method requires the computation of fewer points than the method of conformal mapping because these points may be arbitrarily placed on the airfoil. The method may be applied to isolated airfoils and to airfoils in cascade. For the cascade, the inflow and discharge velocities and a velocity distribution on the surface of an airfoil are given and the shape of the airfoil is determined. In some cases, the spacing of the blades is preassigned, which places a condition on the assumed velocity distribution. Once the airfoil shape has been evolved, the velocity distribution may be computed for any angle of attack by the method described in appendix A. The method of this paper was developed at the NACA Cleveland laboratory during 1946.

THEORY

OUTLINE OF METHOD

In reference 5, it is demonstrated that the two-dimensional potential flow about a body in a uniform stream can be represented by substituting for the body a sheet of vortices along its boundary. The vortex strength per arc length at any point is equal to the magnitude of the velocity at that point. A proof of this relation for the case of the cascade is given in appendix B. The problem of finding a shape with a prescribed velocity distribution when placed in a stream can then be stated: Given a vortex distribution, to find a contour which satisfies the condition that it will be a streamline in the flow field induced by the uniform flow and the vortices distributed on the contour.

The procedure of finding the shape begins by choosing an approximate shape and distributing the vortices on it. The stream function of the flow induced by the vortices and the uniform stream is computed at points on the boundary of the assumed shape. If this stream function is constant, the assumed shape is correct. Variations of the stream function are a measure of the deviation of the assumed shape from the correct one. These variations are used to distort the original shape into a new shape whose stream function is more nearly constant. The process is repeated until the variations become negligible. In the process of shape adjustment, the velocity is altered on the pressure surface.

DERIVATION OF EQUATIONS FOR THE STREAM FUNCTION

Isolated airfoil.—The complex or reflected velocity $w'(z)$ (which is the derivative of the complex potential function $w(z)$) induced at the point $z=x+iy$ by a vortex of strength k located at $z_o=x_o+iy_o$ is

$$w'(z)=\frac{k}{2\pi i}\,\frac{1}{z-z_o}$$

(A summary of the principal symbols used in this report is given in appendix C.)

The complex velocity $w'(z)$ induced by a uniform stream with complex velocity w_u' and a distribution of vortex strength per unit length $\gamma(z_o)$ along a curve with coordinates z_o, is

$$w'(z)=w_u'+\frac{1}{2\pi i}\int\frac{\gamma(z_o)\,ds_o}{z-z_o} \qquad (1)$$

where ds_o is the element of arc length along the curve. The complex potential at the point z is the integral of $w'(z)$ with respect to z, namely

$$w(z)=zw_u'+\frac{1}{2\pi i}\int\gamma(z_o)\log(z-z_o)\,ds_o \qquad (2)$$

From reference 1 (notation modified),

$$\gamma(z_o)\,ds_o=w'(z_o)\,dz_o=dw(z_o)=d\varphi(z_o)+i\,d\psi(z_o)$$

where

φ velocity potential, $R[w(z)]$

ψ stream function, $I[w(z)]$

When equation (2) is applied to obtain the complex potential function at any point z in the flow field, the integration must be carried out along the boundary of the body. Because this curve is a streamline, $d\psi=0$ and, therefore, equation (2) becomes

$$w(z)=zw_u'+\frac{1}{2\pi i}\int\log(z-z_o)\,d\varphi(z_o) \qquad (2a)$$

The imaginary part of equation (2a) is the stream function at the point z,

$$\psi=-xV_y+yV_x-\frac{1}{2\pi}\int\log\sqrt{(x-x_o)^2+(y-y_o)^2}\,d\varphi(z_o) \qquad (3)$$

where

V_y y-component of uniform stream velocity V

V_x x-component of uniform stream velocity V

It is convenient to use the arc length along the airfoil as a parameter. If (x,y) is a point on the airfoil boundary, then s will denote the arc length there; similarly, s_o will denote the arc length at (x_o, y_o). The vortex at s_o on the airfoil influences the stream function at the point s on the ai The stream function induced at (x,y) by a vortex of strength at (x_o, y_o) is

$$f_1(z,z_o)=\frac{1}{4\pi}\log[(x-x_o)^2+(y-y_o)^2]$$

A plot in the (x,y) plane of curves for a constant f_1 consists of concentric circles with center at (x_o, y_o).

The velocity at the point s_o on the airfoil is the direct derivative $\varphi'(s_o)$ of the potential along the strea If the velocity along the airfoil has been specified an airfoil shape has been assumed, the resultant stream tion along the boundary of the airfoil can be approxin by using the approximate shape in evaluating the integ

$$\psi(s)=\psi_u(s)-\int_0^l f_1(s,s_o)\varphi'(s_o)\,ds_o$$

where

$\psi_u(s)$ stream function at (x,y) due to uniform stream, $-xV_y$

l total arc length of airfoil

All variables are expressed in terms of the arc-length meters s and s_o. The integral in equation (5) can be e ated either numerically or graphically over the entire of integration except in the region where a ($\equiv s-s_o$) is s for in this region $f_1(s,s_o)$ becomes infinite. This portio the integral can be evaluated by approximating the a boundary by a line segment. Then,

$$f_1(s,s_o)\approx\frac{1}{4\pi}\log(s-s_o)^2$$

The prescribed velocity can be given in this region, w may be defined by $s-a\leqq s_o\leqq s+a$, by a Taylor's seri a function of s_o about the point s.

$$\varphi'(s_o)=\varphi'(s)+\varphi''(s)(s_o-s)+\frac{\varphi'''(s)}{2!}(s_o-s)^2+\cdots$$

where the primes indicate derivatives with respect The integral is then

$$\int_{s-a}^{s+a}f_1(s,s_o)\varphi'(s_o)\,ds_o=\int_{s-a}^{s+a}\frac{1}{4\pi}\log(s_o-s)^2[\varphi'(s)+\varphi''(s)(s_o-s)+\cdots]\,ds_o$$
$$=\frac{1}{\pi}\left[a\varphi'(s)\,(\log a-1)+\frac{a^3\varphi'''(s)}{3!}\left(\log a-\frac{1}{3}\right)+\cdots\right]$$

In most cases, only the first term need be used in equation (6). The same type of approximation can be used to eval a portion of the integral if the opposite side of the airfoil comes in the neighborhood of the point (x,y).

A more general equation applicable to a segment that does not pass through s is:

$$\frac{1}{4\pi}\int_{p+b}^{p+c}\log[(x-x_o)^2+(y-y_o)^2]\varphi'(s_o)\,d(s_o)=\frac{1}{4\pi}\Bigg\{\varphi'(p)\left[c\log(h^2+c^2)-b\log(h^2+b^2)-2(c-b)+2h\tan^{-1}\frac{h(c-b)}{h^2+bc}\right]+$$
$$\frac{\varphi''(p)}{2!}[(h^2+c^2)\log(h^2+c^2)-(h^2+b^2)\log(h^2+b^2)-(c^2-b^2)]+$$
$$\frac{\varphi'''(p)}{3!}\left[c^3\log(h^2+c^2)-b^3\log(h^2+b^2)-\frac{2}{3}(c^3-b^3)+\right.$$
$$\left.2h^2(c-b)-2h^3\tan^{-1}\frac{h(c-b)}{h^2+bc}\right]+\cdots\Bigg\}$$

where h is the perpendicular distance from s to the segment, $s_o=p$ locates the foot of the segment, $(p+b)$ and $(p+c)$ are the limits of the integration of s_o, and approximately,

$$\varphi'(p)=\varphi'(p+b)-b\varphi''(p+b)+\frac{b^2}{2}\varphi'''(p+b)$$
$$\varphi''(p)=\varphi''(p-b)-b\varphi'''(p-b)$$
$$\varphi'''(p)=\varphi'''(p-b)$$

Equation (6a) may be used when the line segment is not of equal lengths on either side of the perpendicular foot or when $\varphi'(s)$ or its derivatives are discontinuous at either $(p+b)$ or $(p+c)$. If $a=c=-b$ and $h=0$, equation (6a) reduces to equation (6). The size of a, b, or c is determined by the requirements that the segment in question be nearly straight (the approximation is of the second degree) and that $\varphi'(s_o)$ be accurately represented by a Taylor's series expansion of few terms.

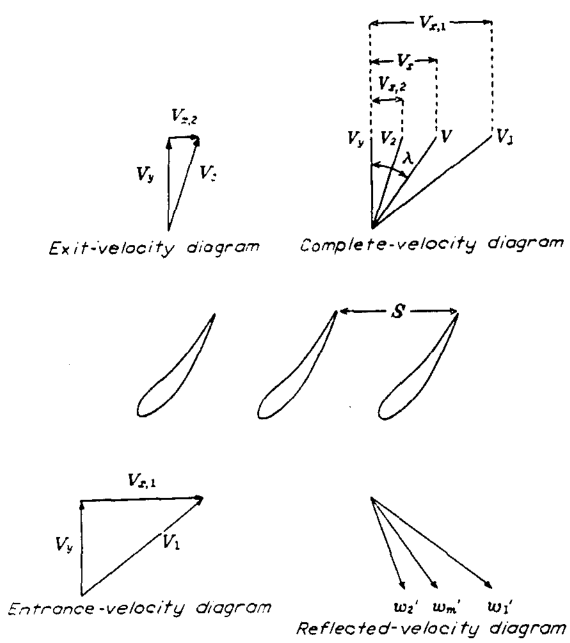

FIGURE 1.—Notation for cascade flow.

Airfoils in cascade.—The expression for the complex potential for the flow about a cascade of airfoils is derived in appendix B. The notation is defined in figure 1. The equation that corresponds to equation (2a) for isolated airfoils is for a cascade of airfoils

$$w(z)=zw_m'+\frac{1}{2\pi i}\int\log\left[\sin\frac{\pi}{S}(z-z_o)\right]d\varphi(z_o) \tag{7}$$

where

w_m' mean stream velocity, which is one-half the sum of complex (reflected) velocities upstream and downstream of cascade, V_x-iV_y

S distance between successive airfoils in cascade

The mean velocity w_m' corresponds to the uniform velocity w_u' of the isolated airfoil flow.

The term zw_m' is the complex potential function resulting from the mean flow. In the integral, the element $d\varphi$ indicates the vortex-element strength and $\log\,[\sin\,(\pi/S)\,(z-z_o)]$ represents the complex potential at the point z caused by an infinite row of unit vortices at $z_o\pm nS$ where $n=0$, 1, 2, ... The imaginary part of equation (7) is the stream function.

$$\psi(s)=\psi_m(s)-\int_{s_o=0}^{s_o=l}f_2(s,s_o)\;d\varphi(s_o) \tag{8}$$

where

$$f_2(s,s_o)=\frac{1}{4\pi}\log\left[\sin^2\frac{\pi}{S}(x-x_o)+\sinh^2\frac{\pi}{S}(y-y_o)\right]$$

is expressed in arc-length parameters and $\psi_m(s)$ is the stream function at (x,y) induced by a mean stream whose complex velocity is w_m'; that is,

$$\psi_m=-xV_y+yV_x$$

The values of $(x\text{-}x_o)/S$ and $(y\text{-}y_o)/S$ for various values of f_2 are given in table I. A plot of $x\text{-}x_o$ and $y\text{-}y_o$ for constant values of $f_2(z,z_o)$ is shown in figure 2. These curves may be

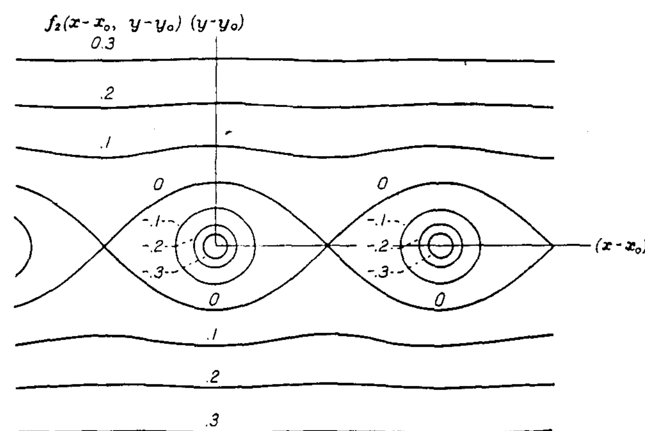

FIGURE 2.—Plot of curves for constant $f_2(x-x_o,\ y-y_o)$.

interpreted as the streamlines of the flow induced by an infinite row of vortices of unit strength located at the points $(x_o\pm nS,\ y_o)$, where $n=0$, 1, 2, ... In the region of a vortex, the streamlines are nearly circles; that is, the flow is nearly that induced by an isolated vortex. At a distance from the vortex row, the streamlines are parallel lines, as in the flow pattern induced by a continuous uniform distribution of vorticity along a straight line instead of a row of discrete vortices. The velocities on the two sides of such a vortex line are of equal magnitude but opposite in direction.

This behavior of f_2 for large $|y-y_o|/S$ and also for small $\frac{(y-y_o)^2+(x-x_o)^2}{S^2}$ can be described as follows: When both $(x-x_o)/S$ and $(y-y_o)/S$ are small,

$$f_2(z,\,z_o)\approx\frac{1}{4\pi}\log\frac{\pi^2}{S^2}\left[(x-x_o)^2+(y-y_o)^2\right] \tag{9}$$

which differs from $f_1(z,\,z_o)$ only by a constant. For large values of $|y-y_o|/S$, irrespective of $(x-x_o)/S$ and a constant term,

$$f_2(z,\,z_o)\approx\frac{|y-y_o|}{2S} \tag{10}$$

which is the stream function of a uniform stream parallel to the x-axis.

Equation (8) can be used for computing the stream function along the boundary of an airfoil in cascade j equation (5) is used for the isolated airfoil. The integral over the range in the neighborhood of the point s is obtai using equation (9) for $f_2\ (s,s_o)$. The result, derived in the same manner as equation (6), is

$$\pi \int_{s-a}^{s+a} f_2(s, s_o)\varphi'(s_o)\ ds_o = \left\{ a\varphi'(s)\left[\log\left(\frac{\pi}{S}a\right)-1\right]+a^3\,\frac{\varphi'''(s)}{3!}\left[\log\left(\frac{\pi}{S}a\right)-\frac{1}{3}\right]+\ \cdot\ \cdot\ \cdot \right\}$$

The more general equation (6a) is modified for cascades by multiplying the argument of all logarithms by the factor π^2/S^2.

ADJUSTMENT OF SHAPE

If the stream function for the assumed airfoil has been computed and has been found to vary, the shape must then be adjusted to give a more nearly constant stream function. The shape changes are made by rotation of the body plus displacement of the individual points normal to the mean stream. The rotation is used to place the front stagnation point properly.

Rotation of the airfoil.—In the formula for computing the stream function of an isolated airfoil, the contribution of a vortex element at (x_o, y_o) to the stream function of a point at (x, y) is dependent merely on the distance between the two points. Consequently, if the entire airfoil is rotated, the effect of the boundary vortices on the stream function at any point on the airfoil boundary will not change. The effect of the blade rotation on the stream function along the boundary is therefore determined by the change in relative position of the points in the uniform stream. The first adjustment in shape is a rigid rotation of the airfoil in order to obtain a more nearly constant stream function along its boundary.

If the airfoil is rotated through an angle β, the stream function is so changed that $\psi\ (s)$ is a function of β and s and may be written $\psi\ (s, \beta)$. When $\beta=0$, $\psi\ (s, 0)$ is the o stream function before rotation. After rotation th stream function $\psi\ (s, \beta)$ may be expanded in a Taylor's about the point $\beta=0$,

$$\psi(s,\beta)=\psi(s,0)+\beta\left[\frac{\partial\psi(s,\beta)}{\partial\beta}\right]_{\beta=0}+\ .\ .\ .$$

Only the first two terms in this series will be used bec is assumed to be small. The angle β is to be determi the minimum mean-square deviation of the stream fu from its mean value. Because the object of the rota essentially to adjust the shape of the nose, the rotation also be made to reduce the root-mean-square deviation stream function to a minimum for a portion of the including the nose.

The mean value of the stream function at any ang

$$\overline{\psi}(\beta)=\frac{1}{l}\int_0^l \psi(s,\beta)\ ds=\frac{1}{l}\int_0^l \left\{\psi(s,0)+\beta\left[\frac{\partial\psi}{\partial\beta}(s,\beta)\right]_{\beta=0}\right\}\ d\cdot$$

The difference between the new stream function $\psi\ (s, \beta$ its mean value $\overline{\psi}\ (\beta)$ is squared and integrated to ob measure of the variation of $\overline{\psi}\ (s,\ \beta)$ from the mean va the new angle. The condition for obtaining a min root-mean-square deviation by adjusting β is

$$\begin{aligned}
0&=\frac{d}{d\beta}\int_0^l\left[\psi(s,\beta)-\overline{\psi}(\beta)\right]^2 ds=\frac{d}{d\beta}\int_0^l\left[\overline{\psi}(s,0)+\beta\,\frac{d\psi(s,0)}{d\beta}-\overline{\psi}(\beta)\right]^2 ds\\
&=\int_0^l 2\left[\psi(s,0)+\beta\,\frac{d\psi(s,0)}{d\beta}-\overline{\psi}(\beta)\right]\left[\frac{d\psi(s,0)}{d\beta}-\frac{d\overline{\psi}(\beta)}{d\beta}\right] ds\\
&=2\int_0^l \frac{d\psi(s,0)}{d\beta}\left[\psi(s,0)+\beta\,\frac{d\psi(s,0)}{d\beta}-\overline{\psi}(\beta)\right] ds-\\
&\qquad 2\,\frac{d\overline{\psi}(\beta)}{d\beta}\int_0^l\left[\psi(s,0)+\beta\,\frac{d\psi(s,0)}{d\beta}-\overline{\psi}(\beta)\right] ds
\end{aligned}$$

The second integral vanishes by virtue of equation (11), which may also be used to eliminate $\overline{\psi}\ (\beta)$ from the remaining term. The solution for β is

$$\beta=\frac{\int_0^l\psi(s)\,\frac{d\psi(s,0)}{d\beta}\,ds-\frac{1}{l}\left[\int_0^l\psi(s)\,ds\right]\left[\int_0^l\frac{d\psi(s,0)}{d\beta}\,ds\right]}{\frac{1}{l}\left[\int_0^l\frac{d\psi(s,0)}{d\beta}\,ds\right]^2-\int_0^l\left[\frac{d\psi(s,0)}{d\beta}\right]^2 ds} \tag{14}$$

In order to apply equation (14), $d\psi/d\beta$ must be known at points along the boundary of the airfoil. For the isolated airfoil, the contribution of the vortices is unaffected by the rotation and therefore

$$\frac{d\psi}{d\beta}=\frac{d\psi_u}{d\beta}=\frac{d}{d\beta}\left(-xV_y+yV_x\right)=-V_y\frac{dx}{d\beta}+V_x\frac{dy}{d\beta} \tag{15}$$

If the airfoil is rotated about the point (x_c, y_c), equation (15) becomes

$$\frac{d\psi}{d\beta}=\cos\beta\ [(x-x_c)V_x+(y-y_c)V_y]+\sin\beta\ [(x-x_c)V_y-(y-y_c)V_x]$$

where (x, y) are the coordinates of the point before rot: For small values of β, equation (16) reduces to

$$\frac{d\psi}{d\beta}=(x-x_c)V_x+(y-y_c)V_y$$

The choice of (x_c, y_c) will have no effect on the results i case.

When the airfoil in cascade is rotated, the change i position of the vortices of the adjacent blade must be sidered. For the isolated airfoil, it was unnecessary to sider the change in position of the vortices becaus influence of a vortex (equations (3), (4), and (5)) dep on the function f_1, which is constant on circles. The infl of the vortices on the airfoil is therefore independe direction. Because the f_2 contours are not circles, the rotation in cascade does have an effect, which is approximated by considering all closed f_2 curves ($f_2<0$) as circles in order that the effect of all vortices in the region $f_2<0$ may be neglected during rotation. The effect of all vortices in the region $f_2>0$ is estimated by assuming that all the f_2 contours for $f_2>0$ are straight lines uniformly spaced. The flow corresponds to that between two infinite straight parallel vortex sheets of uniform strength per unit length. This flow induced by the vortices in the region $f_2>0$ is in the x-direction, and the direction of the flow induced by the vortices for which $y_o>y$ is opposite in sense to that induced by the vortices for which $y_o<y$.

As the point being considered is changed, the regions for $f_2>0$, $y_o>y$, and $f_2>0$, $y_o<y$ will include different sections of the blades, and hence different vorticity, with the result that the x-velocity component v_x induced by the vortex sheets will vary with the point under consideration. The algebraic sum of the x-component of the uniform flow velocity and the variable x-velocity v_x induced by the vortices in the region $f_2>0$ is to be used like the velocity component V_x in rotation of the isolated airfoil (equation (17)). The quantity V_x in equation (17) is replaced by the corresponding $V_{x,r}=V_x+v_x$. The vortex strength per unit length at any point on the airfoil is equal to $\varphi'(s_o)$ and, therefore, from equation (10) the x-component of the velocity induced by the vortices is $\frac{1}{2S}\int \varphi'(s_o)\ ds_o$, where the integration is carried out over the portion of the airfoil where $f_2(s,s_o)>0$. A distinction must be made between the two regions $y_o<y$ and $y_o>y$ because the induced velocity components have opposite directions.

The computed result of rotating an airfoil in cascade depends upon the choice of (x_c,y_c). In order to minimize the error involved, values of $d\psi/d\beta$ are reduced by choosing (x_c,y_c) as the centroid of the vortex distribution on the airfoil. If the improvement in the mean-square deviation of ψ is small compared with its original value, it may be preferable to omit the rotation of the airfoil because of the error inherent in the approximation for $d\psi/d\beta$. The decision should be made chiefly on how ψ varies at the airfoil nose and whether it is approaching a constant value in this region with successive corrections of the shape.

Distortion of the shape.—The stream function computed after the isolated airfoil has been rotated will, in general, still vary along the boundary. This variation can be reduced by distorting the shape of the airfoil. If the distortion is small, the change in distance between any two points on the boundary will be small, although the change in the direction of a segment joining those points may be considerable. The effect of the distortion on the contribution to the stream function of the vortices on the boundary is consequently neglected. The largest effect of the distortion will be to change the position of the boundary points in the uniform stream. The airfoil is therefore distorted in such a manner that the change in the contribution of the uniform stream to the stream function will eliminate the variations in stream function. For points directly opposite each other on the airfoil, the change in distance will be of the same order of magnitude as the distortion. Consequently, distortions that result in change of thickness of the airfoil converge very slowly because of the inaccuracy of the fundamental assumption on which the correction is based.

Thus, when the stream function along the boundary of the isolated airfoil is known, some number is arbitrarily chosen as the desired constant value of the stream function. If $\Delta\psi=\psi-\overline{\psi}$ is the difference between the computed stream function at a point and the desired constant, the point is moved a distance $-\Delta\psi/V$ perpendicular to the direction of the mean stream, where the direction of increasing uniform stream function is taken as positive. The airfoil in a cascade is distorted in the same manner, by using the varying resultant local mean stream velocity $\sqrt{V_{x,r}^2+V_y^2}$; corrections are made with $\overline{\psi}$ equal to the mean value of ψ on the airfoil.

COMPUTATIONAL PROCEDURE FOR CASCADES

CHOICE OF VELOCITY DISTRIBUTION

Several factors influence the choice of the velocity distribution for which an airfoil is to be found. Especially in rotors, sturdy blades are required. Long thin tail sections must be avoided and where high rotative speeds and stresses occur, overhang of thin sections is likely to induce blade failure. The radial distribution of airfoil cross-sectional area is also fundamental in determining the blade-root stresses. Overhang can be reduced by proper choice of the velocity diagrams for the sections, but the other factors are influenced chiefly by the thickness of the section.

The desired thickness may be attained by first assuming a blade shape and spacing and by then using the stream-filament method of reference 6 to compute the velocity distribution over a portion of the airfoil that determines the thickness. The spacing may be regarded as fixed but the curvature can be adjusted if local velocities are too high for the desired thickness. This computed velocity will then serve as a guide to the choice of an airfoil velocity distribution, which should be chosen to avoid high velocity peaks and steep negative gradients. If the average of the velocities on opposite sides of the blade camber line is retained in the modification of the velocity distribution computed from the stream-filament method, the thickness will also be retained.

Because of the irrotationality of the fluid motion, the velocity integral or circulation around the airfoil must be equal to that around a blade but over a width equal to one blade space. Therefore,

$$\int \varphi'(s)\ ds=\Gamma=S(V_{x,1}-V_{x,2})$$

where

- Γ circulation about airfoil
- $V_{x,1}$ tangential velocity entering cascade
- $V_{x,2}$ tangential velocity leaving cascade

This relation places a condition on the assumed velocity distribution.

If the computations thus far have been made in order to select a velocity distribution for the airfoil cascade in a compressible fluid flow, an equivalent velocity distribution for the flow of an incompressible fluid must be determined before the blade shape can be computed by any method based on incompressible-flow theory. For subcritical flows, the directions of the inflow and discharge velocities are nearly the same for compressible and incompressible flows, but for incompressible flow the component normal to cascade axis is the same upstream and downstream. The Kármán-Tsien compressibility correction (reference 7) or that of Garrick and Kaplan (reference 8) may be applied to the velocity on the blade surface to estimate roughly the corresponding incompressible-flow velocity distribution. The resulting velocity distribution in any case must satisfy the circulation condition. This procedure does not give an exact solution for compressible flows, but the resultant compressible flow will have approximately the desired characteristics of low pressure gradients and no high velocity peaks.

COMPUTATION OF AIRFOIL SHAPE FROM THE CHOSEN VELOCITY DISTRIBUTION

The numerical computation of the quantities involved in the preceding analysis, particularly the function f_2, is extremely laborious when tables of $f_2(s,s_o)$ are used. Most of the computations are therefore executed graphically. In the cascade example, the air was assumed to enter the cascade at an angle of 45° from the cascade axis and to leave at an angle of −30° from the cascade axis. The prescribed velocity distribution is given in figure 3(a). The value of the lift coefficient for this airfoil is 3.1. The shapes of the isolated airfoil and the airfoil in cascade are computed by the following steps:

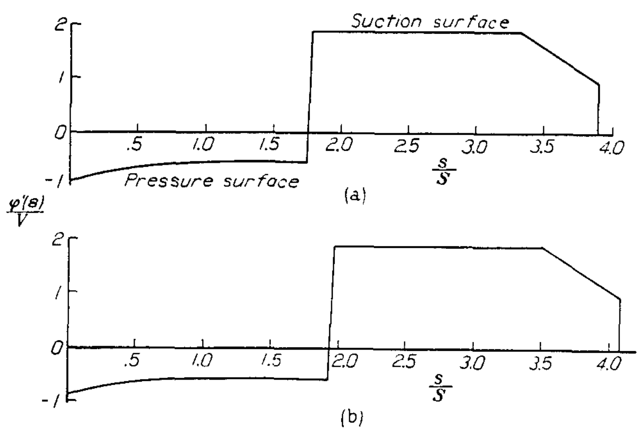

(a) Initial airfoil.
(b) Final airfoil.

FIGURE 3.—Prescribed velocity distribution for thick airfoil in cascade.

1. Curves for constant f_1 for the isolated airfoil, or constant f_2 (fig. 2) for the airfoil in cascade, are drawn. This diagram should be made on some transparent material that will change neither in size nor shape. The coordinates of the curves for constant f_2 are given in table I.

2. A desired velocity $\varphi'(s)$ is chosen as a function of the arc length of the airfoil (fig. 3(a)). An airfoil shape having the desired total arc length is assumed and is drawn to the same scale as the plot of f_1 or f_2. The drawing is made on grid paper and, in the case of a cascade, the x-axis coincides with the cascade axis (fig. 4).

3. The velocity distribution $\varphi'(s)$ is integrated to obtain the velocity potential $\varphi(s)$. This function is plotted on the same chart as the assumed airfoil shape for the correspo y-coordinate, as shown in figure 4, by plotting both

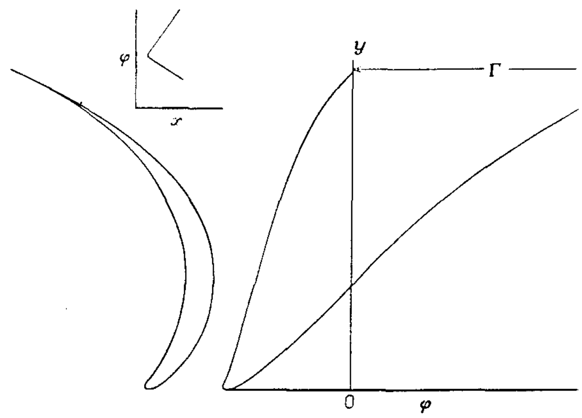

FIGURE 4.—Plot of airfoil and velocity potential for use in computation.

the y-coordinate of the airfoil against s on a suppleme graph. In regions of the airfoil where y varies little w that is, where the airfoil boundary is parallel to the x-dire φ should be plotted against x in the same manner, as s in figure 4.

4. In order to find the stream function at a point on the airfoil, f_2 (s,s_o) must be plotted as a function of to evaluate the quantity $\int f_2(s,s_o)\, d\varphi(s_o)$ of equatio If the chart of f_2 is superimposed on the airfoil with on tex center overlying the point (x,y), the value of f_2 m read at (x_o,y_o) and the corresponding value of $\varphi(x_o,y_o)$ also be read from the plot of $\varphi(x_o,y_o)$. The value of f is the same as would have been obtained by centerin chart on (x_o,y_o) because of the symmetry of the fun A succession of values of φ and f_2 are obtained in this fa for various positions (x_o,y_o) that intersect the f_2 con and a plot of these points (f_2,φ) may be made for the ass position (x,y). This procedure is illustrated in figure a particular point (x,y) on which the f_2 chart is cen The readings for a particular (x_o,y_o) are shown by the arr lines. The points 1 to 6 on the blade are shown o corresponding f_2 curve. The discontinuity of φ bet points 1 and 6 is the circulation. The discontinuity bet 4 and 5 represents the region where f_2 approaches $-\infty$

5. The proper method of integration then proceeds 1 through 6 to 7 and then to the origin, with const from 4 to 5. The region from 4 to 5 with f_2 approa $-\infty$ is computed by equation (6) or (6b); the constan assumed to be the radius of the near-circle, which c ponds to the value of f_2 where the discontinuity from 5 occurs.

The total area including this small addition is

$$\int \varphi'(s_o) f_2(s,s_o)\, ds = \int f_2(s,s_o)\, d\varphi$$

which is the stream function due to vortices on the enti of airfoils in cascade. Where $f_2=0$ at the points A, and D (fig. 5), the values of φ are noted as $\varphi_A(s)$, $\varphi_B(s)$, and $\varphi_D(s)$. These values are used in computing the str function change caused by rotating the blade. The stream function at the point (x, y) may now be computed from equation (8) or (5), and

$$\psi_m = -V_y x + V_x y$$

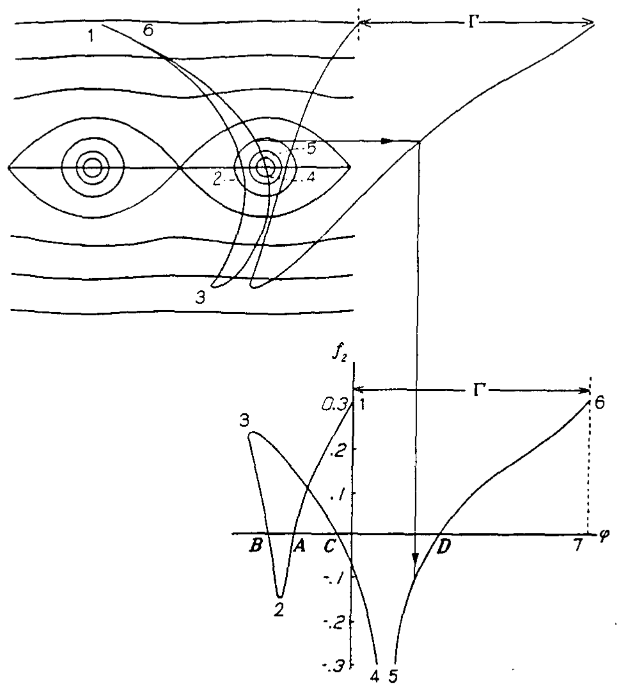

FIGURE 5.—Superposition of figures 2 and 4 to obtain plot of f_2 against φ.

A plot of the stream function (variation from the mean value) is shown in figure 6 for the initially assumed shape. Corresponding points on adjacent airfoils have a difference of $\Delta\psi/V_y S$ equal to 1.0.

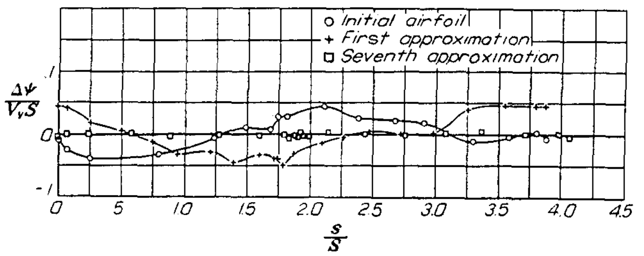

FIGURE 6.—Variation in stream function along initial shape and first and seventh approximations of airfoil cascade.

6. When $\psi(s)$ is known at a sufficient number of points, the airfoil may be rotated as previously described. For the isolated airfoil, equations (14) and (17) may be used directly. For the airfoil in cascade, the coordinates of the centroid of the airfoil must first be computed by

$$x_c = \frac{1}{\Gamma} \oint x\varphi'(s_o)\, ds_o$$

$$y_c = \frac{1}{\Gamma} \oint y\varphi'(s_o)\, ds_o$$

Before equation (17) can be used to compute $d\psi/d\beta$, the variable quantity $V_{x,r}$ must be computed. The vortices in the region $f_2>0$ are considered to be uniformly distributed along the cascade axis and the velocity induced by such a distribution is

$$v_x = \pm \frac{\gamma}{2}$$

where γ is the vortex strength per unit length along the cascade axis for $f_2>0$. Therefore,

$$v_x = \frac{1}{2S} \int \varphi'(s_o)\, ds_o$$

where the integral is to be taken over the regions $f_2>0$. The region $f_2>0$, $y_o>y$ contributed a positive component to v_x, whereas the region $f_2>0$, $y_o<y$ contributes a negative component. The computation is simply carried out by making use of the fact that the integral for v_x is the difference between values of φ at points where $f_2=0$. The values of $\varphi_A(s_o)$, $\varphi_B(s_o)$, $\varphi_C(s_o)$, and $\varphi_D(s_o)$ from step 5 are used at this point to obtain

$$2v_x S = \int \varphi'(s_o)\, ds_o = \varphi_A - \varphi_D + \Gamma - (\varphi_C - \varphi_B) \qquad (18)$$

where Γ is introduced because of the discontinuity in φ at the trailing edge. The sum $\varphi_A - \varphi_D + \Gamma$ gives the effect of the vorticity in the region $f_2(s, s_o)>0$ near the trailing edge, and the term $\varphi_C - \varphi_B$ gives the effect of the vorticity in the region $f_2(s,s_o)>0$ near the leading edge. If either the leading edge or the trailing edge lies in the region $f_2(s,s_o)<0$, only two points of intersection will remain and one of the two groups of terms in equation (18) will vanish. The quantity $\frac{1}{2S}\int \varphi'(s_o)\, ds_o$ is added to the x-component of the original uniform stream velocity and the quantity $d\psi/d\beta$ of equation (17) may be computed for a number of points and the angle β computed from equation (14), using the values of (x_c,y_c) just determined. After these computations have been made, the airfoil is rotated through the angle β, and the value $\psi+\beta\frac{d\psi}{d\beta}$ is assigned as the value of the stream function of the point after rotation.

7. A value of $\psi(s)$ is known at points along the airfoil boundary. The mean value over the airfoil $\bar{\psi}$ is subtracted from ψ leaving $\Delta\psi$. For the isolated airfoil, no subtraction is necessary. Each point is moved a distance $-\frac{\Delta\psi}{\sqrt{V_{x,r}^2+V_y^2}}$ in the direction perpendicular to the velocity computed in step 6. The curve joining the points in their new positions is the adjusted airfoil.

8. The total arc length of the adjusted airfoil will be different from the original one, in general, although local changes in length will be negligible. The airfoil is so scaled that the length of the suction side is the same length as it was before distortion because this surface is the critical surface of the airfoil. This process will result in a change in length of the pressure side. The velocity over the pressure side $\varphi'(s)$

821313—49——2

must then be altered in such a manner that the difference in potential between the two stagnation points remains the same. As a result, the quantities that retain specified values are the length and the velocity distribution on the suction side and the circulation around the airfoil. The entire procedure is repeated with the adjusted shape until the variations in the stream function result in very little change in the shape of the airfoil.

DISCUSSION OF EXAMPLES AND TECHNIQUES

For the example being computed, the stream functions obtained for the initially assumed shape and the first and seventh approximations are plotted against the arc length (fig. 6), which is taken as zero at the trailing edge and proceeds counterclockwise around the airfoil as shown in figure 7. The fact that $\Delta\psi$ for the initial shape is positive over the first half of the arc length and negative over the second half indicates that it is too thick because the required distortion in shape will make it thinner. The change in thickness results in a change in velocity distribution over the pressure side of the airfoil in order to maintain the desired circulation. The velocity that was originally assumed, which is equal to the vorticity per unit length distributed on

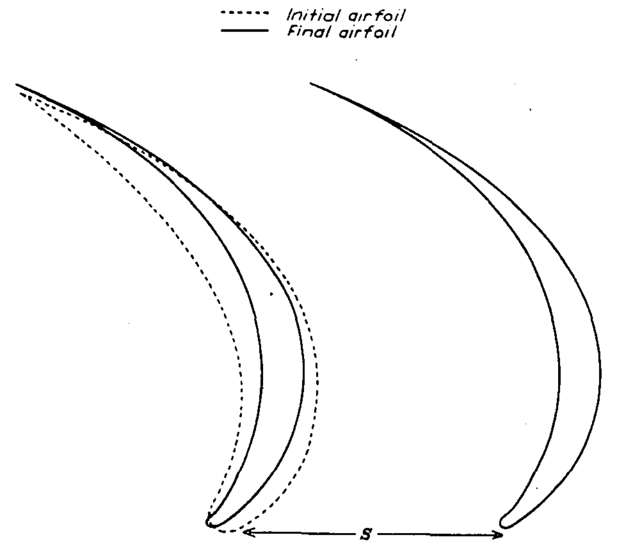

FIGURE 7.—Initial shape and final approximation of thick airfoil showing cascade spacing.

the initial airfoil, is shown in figure 3 (a) and the velocity over the final shape in figure 3 (b). The length of the pressure side has increased and the velocity has decreased in the portion of 1:1.1.

Over the section of the airfoil that has collapsed ' thickness, the surface velocities of figure 3 (b) may n been obtained, but the loading (circulation per u length), which is the difference in the velocities on o sides, has been realized. In practice, this collapse vented by increasing the assumed velocity on the surface.

If the initially assumed airfoil shape has a thickne differs considerably from the correct one, the process o adjustment will converge rather slowly. The labor reduced, however, by computing the stream functio few points on the airfoil and locating these points to mine the thickness. This procedure is followed for t few approximations until the thickness of the airfoil i accurate. The stream function is then computed larger number of points, particularly near the leadin in order to get more detail of the shape.

Arbitrary specification of a velocity distributio result, not in a physically real airfoil, but in a f shape or a collapsed shape (zero thickness over a por the blade). The velocity distribution must then be m to obtain a real shape; these modifications should be s to keep the desirable properties of the original distri Velocity peaks and steep velocity gradients, which t occur on the suction side of an airfoil, are to be a If the airfoil collapses, the vorticities of the two sides t cancel each other and the remaining vorticity represe difference in velocity across the thin airfoil rather th velocity along the boundary.

The method was also applied to the design of a thin (camber line) in a cascade. The vortex distribu equivalent to load distribution (difference in velocity the airfoil) rather than velocity as in the case of a airfoil. The velocity diagram for the cascade and the load distribution for the thin airfoil are shown in fi The value of the lift coefficient of the resultant airfoil

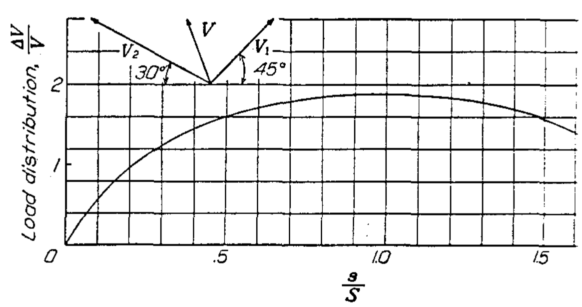

FIGURE 8.—Velocity diagram for cascade and prescribed load distribution for thin cascade.

The initial shape was obtained by assuming zero spacing between the airfoils. The initial shape and the first and third approximations to the airfoil shape are shown in figure 9.

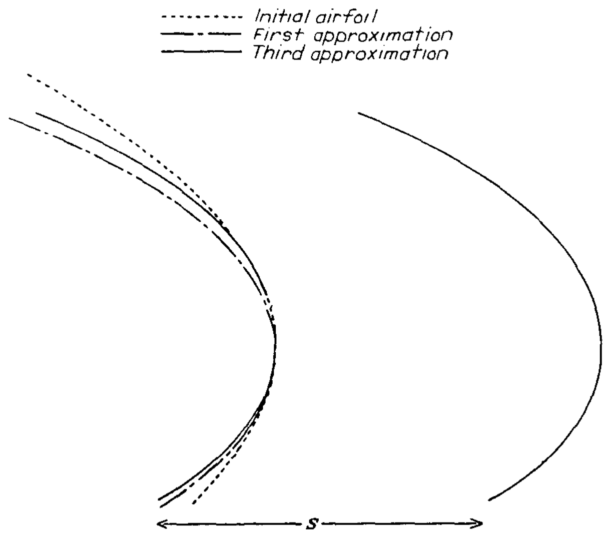

FIGURE 9.—Assumed shape and first and third approximations of thin airfoil showing cascade spacing.

The second and third approximations differ very little. The third approximation is redrawn in this diagram to show the spacing between airfoils. The convergence of the method is shown graphically in figure 10. The variation $\Delta\psi$ of the

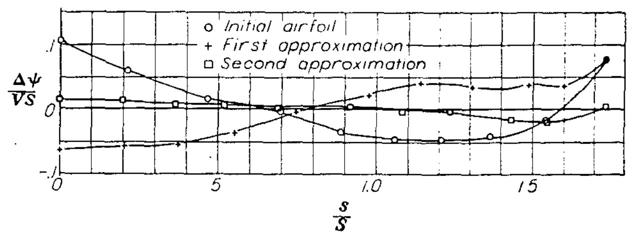

FIGURE 10.—Variation in stream function for successive approximation of thin airfoil in cascade.

stream function from its mean is divided by VS to make it dimensionless and is plotted against the arc length along the airfoil where $s=0$ at the trailing edge. The stream function computed on the second approximation is nearly constant, which gives the third approximation almost the same shape as the second one. The rapid adjustment of camber contrasts with the slow adjustment of thickness.

FLIGHT PROPULSION RESEARCH LABORATORY,
NATIONAL ADVISORY COMMITTEE FOR AERONAUTICS,
CLEVELAND, OHIO, *March 4, 1947.*

APPENDIX A

VELOCITY DISTRIBUTION ON THE DERIVED AIRFOIL AT DIFFERENT FLOW ANGLES

Conformal mapping.—When an airfoil is given, the velocity distribution over its surface must frequently be found at different angles of attack. This problem may be solved by the method of conformal mapping, which consists in mapping the region exterior to the airfoil on the exterior of a circle. The velocity around the airfoil is obtained from the known velocity around the circle. Procedures for finding the function that maps a given airfoil into a circle are presented in references 1 and 9 for the isolated airfoil and references 3 and 10 for the airfoil in cascade.

In general, the procedure for finding the mapping function of an airfoil is a laborious one. But when, as in the present case, the velocity distribution over the airfoil at a particular angle of attack is known, the correspondence between points on the airfoil and on the circle, and hence the flow velocity at other angles of attack, can be obtained very easily. Indeed, the correspondence of points and the velocities for various angles of attack can be obtained by the method given in reference 11 from the initial data without knowing the airfoil shape, because the complex potentials of the airfoil plane and the mapping-circle plane are equal. Before the airfoil is designed it is therefore possible to check whether the airfoil to be computed will be satisfactory under conditions different from the design condition.

Isolated airfoil.—The flow about any airfoil shape can be mapped on the flow about a unit circle in such a way that corresponding points have the same potential. The flow about the airfoil is given and the potential function $\varphi(s)$ at each point is computed. If the potential function on the airfoil is computed by integrating the velocity from the stagnation point at the trailing edge in a counterclockwise direction around the airfoil oriented as in figure 1, the potential will be zero at the trailing edge, decrease to a minimum φ_{min} at the stagnation point at the leading edge, and then increase to a value equal to the circulation Γ at the trailing edge. The corresponding flow about the circle is determined by the conditions that it must have the same values of φ_{min} and Γ for a correspondence to exist between all airfoil and circle points. If θ_T is the central angle of the stagnation point on the circle that corresponds to the trailing edge of the airfoil,

$$\frac{\pi\varphi_{min}}{\Gamma}=-(\cot\theta_T+\theta_T+\pi/2) \tag{A1}$$

Equation (A1) can be solved numerically for θ_T because all the other quantities are known. The velocity at infinity in the circle plane V_c can then be determined from the Kutta-Joukowsky condition, which requires that θ_T be a stagnation point; that is,

$$V_c=-\frac{\Gamma}{4\pi\sin\theta_T} \tag{A2}$$

The velocity potential at points on the circle is

$$\varphi_c=-2V_c\cos\theta+\frac{\Gamma\theta}{2\pi}+2V_c\cos\theta_T-\frac{\Gamma}{2\pi}\theta_T$$

The quantity $2V_c\cos\theta_T-\frac{\Gamma}{2\pi}\theta_T$ is a constant that is subtr

in order to make $\varphi_c=0$ at the stagnation point corres ing to the trailing edge.

The correspondence of points on the airfoil with poi the circle is obtained by associating points where $\varphi(s$ The velocity on the circle at a uniform stream flow angl

$$v_c(\theta,\alpha)=2V_c\,[\sin(\theta+\alpha)-\sin(\theta_T+\alpha)]$$

The nature of the conformal transformation is such tha ratio of the velocity at a point on the airfoil to the vel at the corresponding point on the circle is independe angle of attack. Therefore, the velocity $\varphi_\alpha'(s)$ on the a at flow angle α is

$$\frac{\varphi_\alpha'(s)}{v_c(\theta,\alpha)}=\frac{\varphi'(s)}{v_c(\theta,0)}$$

where the design flow angle is taken as zero. Equation can be used to compute the velocity distribution on th foil except at the two points that were stagnation poi the design angle of attack.

Airfoils in cascade.—The flow about a cascade of ai can be mapped conformally into the flow about a unit with two singular points located on the real axis symn cally with respect to the center of the circle. These sin points correspond to the points at infinity in front o behind the cascade, respectively. In a cascade of air the distance of these points from the center of the cir uniquely determined by the same conditions that deter the flow about the circle in the isolated case; namely circulation per airfoil, the velocity potential at the le edge, the blade spacing, and the upstream and downst flow angles.

The distance from the singular points to the center o circle is denoted by e^K. The flow about the circle is that the location of the stagnation points θ_s is determ by the relation

$$-\frac{\Gamma}{2VS}=\frac{\sin\theta_s}{\sinh K}\cos\lambda+\frac{\cos\theta_s}{\cosh K}\sin\lambda$$

where λ is the angle of inclination of the mean stream t normal to the cascade axis. (See reference 6 for det The quantities Γ, V, S, and λ are known from the flo the cascade plane and therefore equation (A6) provid relation between K and the location of the stagnation po

The velocity potential at any point on the circle is

$$\varphi_{c,c}=\frac{VS}{\pi}\left(\sin\lambda\tan^{-1}\frac{\sin\theta}{\sinh K}-\cos\lambda\tanh^{-1}\frac{\cos\theta}{\cosh K}\right)+\frac{\Gamma}{2\pi}\tan^{-1}\frac{\tan\theta}{\tanh K}-$$

$$\left[\frac{VS}{\pi}\left(\sin\lambda\tan^{-1}\frac{\sin\theta_T}{\sinh K}-\cos\lambda\tanh^{-1}\frac{\cos\theta_T}{\cosh K}\right)+\frac{\Gamma}{2\pi}\tan^{-1}\frac{\tan\theta_T}{\tanh K}\right] \tag{A7}$$

where θ_T is the particular value of θ_s corresponding to the trailing edge of the airfoil. The expression in brackets is a constant so chosen that the potential will vanish at the stagnation point corresponding to the trailing edge of the airfoil. In order to map the cascade on the circle, K must be found so that the value of $\varphi_{c,c}$ at θ_N, the stagnation point θ_s corresponding to the leading edge of the airfoil, is equal to φ_{min}, the value of the velocity potential there. The identity

$$\left(\frac{\sin\theta_s}{\sinh K}\right)^2\sinh^2 K+\left(\frac{\cos\theta_s}{\cosh K}\right)^2\cosh^2 K\equiv 1$$

is used to eliminate $\frac{\cos\theta_s}{\cosh K}$ from equation (A6) to give

$$\frac{\sin\theta_s}{\sinh K}=\frac{-\frac{\Gamma}{2VS}\cosh^2 K\sin\lambda\pm\cos\lambda\sqrt{\cosh^2 K-\cos^2\lambda-\left(\frac{\Gamma}{2VS}\right)^2\cosh^2 K\sinh^2 K}}{\cosh^2 K-\cos^2\lambda} \tag{A8}$$

In successive approximations, a value of K is assumed and equations (A8) and (A6) are used to find $\frac{\sin\theta_N}{\sinh K}$, $\frac{\cos\theta_N}{\cosh K}$, $\frac{\sin\theta_T}{\sinh K}$, and $\frac{\cos\theta_T}{\cosh K}$. These values are inserted into equation (A7) to find $\varphi_{c,c}$ at $\theta=\theta_N$. If $\varphi_{c,c}(\theta_N)$ is not equal to φ_{min}, another value of K is chosen, on the premise that $\varphi_{c,c}(\theta_N)$ will decrease as K is decreased. When $\varphi_{c,c}(\theta_N)$ is evaluated, care should be taken to use consistent values of the inverse tangents. After two values of K and $\varphi_{c,c}(\theta_N)$ are determined, interpolation or extrapolation may be used for new values of K.

When K has been found, it is used in equation (A7) to evaluate $\varphi_{c,c}$ at values of θ all around the circle. A point on the circle corresponds to the point on the airfoil where $\varphi(s)=\varphi_{c,c}$. The velocity at the point θ on the circle is

$$v_{c,c}=\frac{VS}{\pi}\frac{\sinh 2K}{\cosh 2K-\cos 2\theta}\left[\cos\lambda\left(\frac{\cos\theta}{\cosh K}-\frac{\cos\theta_T}{\cosh K}\right)+\sin\lambda\left(\frac{\sin\theta}{\sinh K}-\frac{\sin\theta_T}{\sinh K}\right)\right] \tag{A9}$$

and the velocity $\varphi_\alpha'(s)$ on the airfoil at any other mean flow angle $\lambda+\alpha$ is

$$\varphi_\alpha'(s)=v_{c,c}(\theta,\lambda+\alpha)\frac{\varphi'(s)}{v_{c,c}(\theta,\lambda)} \tag{A10}$$

as in the case of the isolated airfoil.

The designed airfoil was mapped on the unit circle by the method described. The constant K, the natural logarithm of the distance from the singular points to the center of the unit circle, is 0.075. The correspondence between points on the airfoil and those on the circle is plotted in figure 11, which shows the arc length of the airfoil as a function of the central angle of the circle. The velocity at any point on the airfoil for any angle of attack α may be obtained from equations (A9) and (A10), the velocity distribution as in figure 3 (b), and the relation between s and θ as in figure 11. The ratio $\frac{\varphi'(s)}{v_{c,c}(\theta,\lambda)}$ is equal to $d\theta/ds$ (radians) and need be computed only once for any given airfoil.

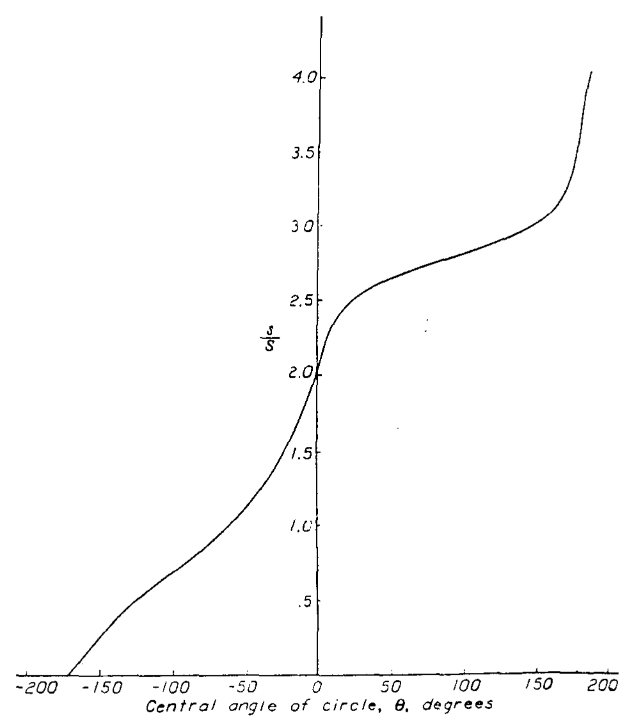

FIGURE 11.—Correspondence between points on airfoil and points on unit circle by conformal transformation.

APPENDIX B

DERIVATION OF THE CASCADE EQUATION

An equation is to be developed for the complex velocity at any point in the field of flow of a fluid past a row of equally spaced, congruent bodies. Coordinates axes are chosen with the origin inside one of the bodies and the x-axis in the direction of the row. (See fig. 12.) The body containing

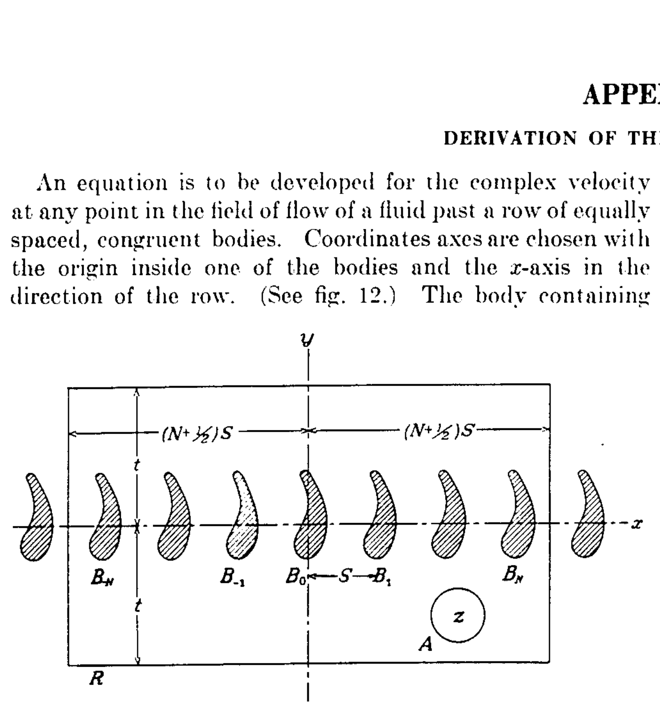

FIGURE 12.—Diagram for derivation of equation for flow about cascade.

the origin is denoted by B_0, bodies along the posit rection of the x-axis by B_1, B_2, . . ., and along the n direction of the x-axis by B_{-1}, B_{-2}, ... A circle A o radius is drawn about the point z where the velocit be determined. A rectangle R is drawn with its cer the origin and its sides parallel to the axes of length (2N and width $2t$, which contains the bodies B_{-N}, . . B_0, B_1, . . . B_N, and the circle A. If a side of the rec intersects one of the bodies, the side may be distorte around the body with no essential change in the The function $w'(z_o)/z_o-z)$ is an analytical function the region inside the rectangle R but outside the bod and the circle A.
Therefore

$$\int_R \frac{w'(z_o)}{z_o-z}\,dz_o-\int_A \frac{w'(z_o)}{z_o-z}\,dz_o-\sum_{n=-N}^{N}\int_{B_n}\frac{w'(z_o)}{z_o-z}\,dz_o=$$

The first integral can be broken up into four int one along each side of the rectangle, namely,

$$\int_R \frac{w'(z_o)}{z_o-z}dz_o=\int_{-(N+1/2)S}^{(N+1/2)S}\frac{w'(x_o-it)}{x_o-it-z}\,dx_o+\int_{-t}^{t}\frac{w'[(N+1/2)S+iy_o]}{(N+1/2)S+iy_o-z}\,idy_o+\int_{(N+1/2)S}^{-(N+1/2)S}\frac{w'(x_o+it)}{x_o+it-z}dx_o+\int_{t}^{-t}\frac{w'[-(N+1/2)S+i\ldots}{-(N+1/2)S+iy_o-\ldots}$$

In an evaluation of these integrals, the function $w'(z_o)$ is periodic, with period S, and approaches a constant value infinitely far from the cascade; that is,

$$w'(x_o+iy_o)\rightarrow w_2' \text{ as } y_o\rightarrow\infty$$

and

$$w'(x_o+iy_o)\rightarrow w_1' \text{ as } y_o\rightarrow-\infty$$

From the last of these conditions, it follows that

$$w'(x_o-it)=w_3'(x_o-it)+w_1'$$

where

$$w_3'(x_o-it)\rightarrow 0 \text{ as } t\rightarrow\infty$$

Therefore, the first integral on the right side of eq (B2) is

$$\int_{-(N+1/2)S}^{(N+1/2)S}\frac{w'(x_o-it)}{x_o-it-z}\,dx_o=w_1'\int_{-(N+1/2)S}^{(N+1/2)S}\frac{dx_o}{x_o-it-z}+\int_{-(N+1/2)S}^{(N+1/2)S}\frac{w_3'(x_o-it)}{x_o-it-z}\,dx_o$$

The first of these integrals is

$$w_1'\int_{-(N+1/2)S}^{(N+1/2)S}\frac{dx_o}{x_o-it-z}=w_1'\log\frac{[(N+1/2)S-it-z]}{[-(N+1/2)S-it-z]}\rightarrow\pi i w_1'$$

as $N\rightarrow\infty$ and $t\rightarrow\infty$, provided that $t/(NS)\rightarrow 0$. The last integral in equation (B3) is

$$\begin{aligned}\int_{-(N+1/2)S}^{(N+1/2)S}\frac{w_3'(x_o-it)}{x_o-it-z}\,dx_o&=\sum_{n=-N}^{N}\int_{(n-1/2)S}^{(n+1/2)S}\frac{w_3'(x_o-it)}{x_o-it-z}\,dx_o\\&=\sum_{n=-N}^{N}\int_{-S/2}^{S/2}\frac{w_3'(x_o-it)}{x_o+nS-it-z}\,dx_o\\&=\int_{-S/2}^{S/2}\frac{w_3'(x_o-it)}{x_o-it-z}\,dx_o+\sum_{n=1}^{N}\int_{-S/2}^{S/2}\frac{2(x_o-it-z)w_3'(x_o-it)\,dx_o}{(x_o-it-z)^2-n^2S^2}\end{aligned}$$

If t is chosen sufficiently large so that $|w_3'(x_o-it)|<\epsilon$, where ϵ is any preassigned positive number, the moduli of the integrals are less than

$$\epsilon\left[\int_{-S/2}^{S/2}\frac{dx_o}{|x_o-it-z|}+\sum_{n=1}^{N}\int_{-S/2}^{S/2}\frac{2|x_o-it-z|\,dx_o}{|(x_o-it-z)^2-n^2S^2|}\right]\leqq\epsilon\left[\int_{-S/2}^{S/2}\frac{dx_o}{\sqrt{(x_o-x)^2+(t+y)^2}}+\sum_{n=1}^{N}\int_{-S/2}^{S/2}\frac{2\sqrt{(x_o-x)^2+(t+y)^2}\,dx_o}{(x_o-x)^2+(t+y)^2-n^2S^2}\right]$$

When $N\rightarrow\infty$, this quantity approaches

$$\epsilon\int_{-S/2}^{S/2}\frac{\pi}{S}\cot\left[\frac{\pi}{S}\sqrt{(x_o-x)^2+(t+y)^2}\right]dx_o$$

This integral is finite and, because ϵ can be made arbitrarily small as $t\rightarrow\infty$, the last integral in equation (B3) approaches zero. Therefore,

$$\int_{-(N+1/2)S}^{(N+1/2)S}\frac{w'(x_o-it)}{x_o-it-z}\,dx_o\rightarrow\pi i w_1'$$

as $t\rightarrow\infty$ and $\frac{t}{NS}\rightarrow 0$. In the same way and under the same conditions,

$$\int_{(N+1/2)S}^{-(N+1/2)S}\frac{w'(x_o+it)}{x_o+it-z}\,dx_o\rightarrow\pi i w_2'$$

The second and fourth integrals on the right side of equation (B2) can be evaluated by combining them. Because w' is periodic,

$$w'[(N+1/2)S+iy_o]=w'[-(N+1/2)S+iy_o]$$

and therefore,

$$\int_{-t}^{t}\frac{w'[(N+1/2)S+iy_o]}{(N+1/2)S+iy_o-z}\,idy_o+\int_{t}^{-t}\frac{w'[-(N+1/2)S+iy_o]}{-(N+1/2)S+iy_o-z}\,idy_o=\int_{-t}^{t}\frac{-2(N+1/2)Sw'[(N+1/2)S+iy_o]}{(iy_o-z)^2-(N+1/2)^2S^2}\,idy_o$$

The velocity $w'[(N+1/2)S+iy_o]$ is bounded for all values of y_o; that is, there is a constant W such that $|w'[(N+1/2)S+iy_o]|<W$. The absolute value of the integral is less than

$$2S(N+1/2)W\int_{-t}^{t}\frac{dy_o}{|(iy_o-z)^2-(N+1/2)^2S^2|}\leqq 2S(N+1/2)W\int_{-t}^{t}\frac{dy_o}{(y_o-y)^2+(N+1/2)^2S^2-x^2}$$

$$=\frac{2S(N+1/2)W}{\sqrt{(N+1/2)^2S^2-x^2}}\left[\tan^{-1}\frac{t-y}{\sqrt{(N+1/2)^2S^2-x^2}}-\tan^{-1}\frac{-t-y}{\sqrt{(N+1/2)^2S^2-x^2}}\right]$$

As $t\rightarrow\infty$ and $\frac{t}{NS}\rightarrow 0$, this quantity approaches zero. It has been shown, therefore, that when $t\rightarrow\infty$ and $\frac{t}{NS}\rightarrow 0$,

$$\int_R\frac{w'(z_o)}{z_o-z}\,dz_o\rightarrow\pi i\,(w_2'+w_1') \tag{B4}$$

By the residue theorem,

$$\int_A\frac{w'(z_o)}{z_o-z}\,dz_o=2\pi i w'(z) \tag{B5}$$

The periodicity of $w'(z)$ implies that

$$\sum_{n=-N}^{N}\int_{B_n}\frac{w'(z_o)}{z_o-z}\,dz_o=\sum_{n=-N}^{N}\int_{B_0}\frac{w'(z_o)}{z_o+nS-z}\,dz_o$$

$$=\int_{B_0}\frac{w'(z_o)}{z_o-z}\,dz_o+\sum_{n=1}^{N}\int_{B_0}\frac{w'(z_o)2(z_o-z)}{(z_o-z)^2-n^2S^2}\,dz_o\rightarrow\int_{B_0}\frac{\pi}{S}w'(z_o)\cot\frac{\pi}{S}(z_o-z)\,dz_o \tag{B6}$$

as $N\rightarrow\infty$.

When equations (B4), (B5), and (B6) are substituted into equation (B1), the expression for the complex velocity is obtained:

$$(z)=\frac{1}{2}(w_1'+w_2')-\frac{1}{2\pi i}\int_{B_0}\frac{\pi}{S}w'(z_o)\cot\frac{\pi}{S}(z_o-z)\,dz_o \tag{B7}$$

The complex potential is obtained from equation (B7) by integrating with respect to z and neglecting the arbitrary constant,

$$w(z)=zw_m'+\frac{1}{2\pi i}\int_{B_0}w'(z_o)\log\sin\frac{\pi}{S}(z-z_o)\,dz_o \tag{B8}$$

where $w_m'=\frac{w_1'+w_2'}{2}$ is the mean stream velocity.

APPENDIX C

SYMBOLS

The principal symbols used throughout the report are listed here for convenience of reference.

$f_1 \equiv$ $\frac{1}{4\pi} \log \left[(x-x_o)^2+(y-y_o)^2 \right]$

$f_2 \equiv$ $\frac{1}{4\pi} \log \left[\sin^2 \frac{\pi}{S} (x-x_o)+\sinh^2 \frac{\pi}{S} (y-y_o) \right]$

K natural logarithm of distance from singular point to center of circle corresponding to cascade airfoil

l total arc length of airfoil

S distance between successive airfoils in cascade

s arc-length parameter corresponding to z

s_o arc-length parameter corresponding to z_o

V magnitude of uniform or mean stream velocity in airfoil or cascade plane (fig. 1)

V_c magnitude of uniform stream velocity in circle plane

V_x x-component of uniform or mean stream velocity V

$V_{x,r}$ resultant local mean stream x-component of velocity V

V_y y-component of uniform or mean stream velocity V

v_c local velocity on circle corresponding to isolated airfoil

$v_{c,c}$ local velocity on circle corresponding to airfoil in cascade

v_x velocity induced by vortices in region $f_2>0$

w complex potential function, $\varphi+i\psi$

w_m' complex velocity of mean stream for airfoil in cascade $\left[w_m'=\frac{1}{2} (w_1'+w_2')=V_x-iV_y \right]$

w_u' complex velocity of uniform stream for isolated airfoil, V_x-iV_y

x real part of z

x_c, y_c coordinates of point about which airfoil is rotated (centroid of vortex distribution for cascade airfoils)

y imaginary part of z

z coordinate of point where stream function is computed, $x+iy$

z_o coordinate of point where vortex is located, x_o+iy_o

α angle of inclination of uniform stream velocity to x-axis

β angle through which airfoil is rotated

Γ circulation about airfoil

$\gamma(z_o)$ vortex strength per unit arc length at z_o

θ central angle of circle

θ_N angle of stagnation point on circle corresponding to leading edge of airfoil

θ_T angle of stagnation point on circle corresponding to trailing edge of airfoil

λ angle of inclination of mean flow to normal to ca axis (fig. 1)

φ velocity potential on airfoil, $R[w(z)]$

$\varphi_A, \varphi_B,$ φ_C, φ_D values of φ at points A, B, C, D, respectively, curve of $\varphi(s_o)$ intersects $f_2(s, s_o)=0$ (See fig.

φ_c velocity potential on circle corresponding to is airfoil

$\varphi_{c,c}$ velocity potential on circle corresponding to air cascade

φ_{min} velocity potential at leading edge of airfoil

ψ stream function, $I[w(z)]$

ψ_m stream function of mean stream of cascade flow

ψ_u stream function of uniform stream flowing isolated airfoil

$\bar{\psi}$ mean value of stream function over airfoil

$\Delta\psi$ variation of stream function, $\psi-\bar{\psi}$

Subscripts 1 and 2 when appended to w', V, and V_x in inflow and discharge values, respectively.

REFERENCES

1. Mutterperl, William: The Conformal Transformation of an into a Straight Line and Its Application to the Inverse Pr of Airfoil Theory. NACA ARR No. L4K22a, 1944.
2. Theodorsen, Theodore: Airfoil-Contour Modifications Bas ε-Curve Method of Calculating Pressure Distribution. ARR No. L4G05, 1944.
3. Mutterperl, William: A Solution of the Direct and Inverse tial Problems for Arbitrary Cascades of Airfoils. NACA No. L4K22b, 1944.
4. Ackeret, J.: The Design of Closely Spaced Blade Grids. R. T. P. Trans. No. 2007, Ministry Aircraft Prod. Schweiz. Bauzeitung, vol. 120, no. 9, Aug. 29, 1942, pp. 103
5. von Mises, Richard, and Friedrichs, Kurt O.: Fluid Dyn Advance Instruction and Research in Mechanics, ch Brown Univ., Summer, 1941, pp. 96–97.
6. Stodola, A.: Steam and Gas Turbines, vol. II. McGraw Book Co., Inc., 1927, pp. 992–994. (Reprinted, Peter (New York), 1945.)
7. von Kármán, Th.: Compressibility Effects in Aerodyna Jour. Aero. Sci., vol. 8, no. 9, July 1941, pp. 337–356.
8. Garrick, I. E., and Kaplan, Carl: On the Flow of a Compre Fluid by the Hodograph Method. I—Unification and Exte of Present-Day Results. NACA Rep. No. 789, 1944.
9. Theodorsen, T., and Garrick, I. E.: General Potential Theo Arbitrary Wing Sections. NACA Rep. No. 452, 1933.
10. Garrick, I. E.: On the Plane Potential Flow past a Symme Lattice of Arbitrary Airfoils. NACA Rep. No. 788, 1944.
11. Gebelein, H.: Theory of Two-Dimensional Potential Flow Arbitrary Wing Sections. NACA TN No. 886, 1939.

TABLE I. COORDINATES OF $f_2(x-x_o,\ y-y_o)$

(a) Values of $(y-y_o)/S$

f_2 ↓ \ $\frac{x-x_o}{S}$ →	0	0.05	0.10	0.15	0.20	0.25	0.30	0.35	0.40	0.45	0.50
−0.40	0.0257										
−.38	.0292										
−.36	.0331										
−.34	.0375										
−.32	.0425										
−0.30	0.0481										
−.28	.0545	0.0229									
−.26	.0618	.0371									
−.24	.0699	.0497									
−.22	.0791	.0621									
−0.20	0.0894	0.0750									
−.18	.1010	.0887	0.0296								
−.16	.1140	.1035	.0620								
−.14	.1286	.1195	.0871								
−.12	.1447	.1369	.1107	0.0392							
−0.10	0.1626	0.1560	0.1344	0.0881							
−.08	.1824	.1768	.1588	.1241	0.0454						
−.06	.2011	.1993	.1844	.1572	.1103						
−.04	.2277	.2236	.2113	.1896	.1558	0.1014					
−.02	.2532	.2198	.2396	.2222	.1966	.1608	0.1096				
0	0.2805	0.2778	0.2694	0.2553	0.2354	0.2096	0.1777	0.1400	0.0969	0.0496	0.0000
.02	.3097	.3074	.3006	.2892	.2737	.2542	.2318	.2081	.1858	.1692	.1629
.04	.3405	.3386	.3331	.3239	.3117	.2968	.2804	.2638	.2491	.2389	.2352
.06	.3728	.3713	.3668	.3595	.3498	.3384	.3260	.3139	.3036	.2965	.2940
.08	.4064	.4052	.4016	.3958	.3881	.3793	.3698	.3608	.3533	.3482	.3464
0.10	0.4412	0.4402	0.4373	0.4327	0.4267	0.4198	0.4126	0.4058	0.4001	0.3964	0.3951
.12	.4769	.4761	.4739	.4702	.4655	.4601	.4545	.4493	.4451	.4423	.4413
.14	.5135	.5129	.5111	.5082	.5045	.5003	.4960	.4920	.4888	.4867	.4859
.16	.5508	.5503	.5488	.5466	.5437	.5404	.5371	.5340	.5316	.5299	.5294
.18	.5886	.5882	.5871	.5853	.5830	.5805	.5779	.5735	.5736	.5724	.5720
0.20	0.6269	0.6266	0.6257	0.6243	0.6225	0.6205	0.6185	0.6167	0.6152	0.6143	0.6140
.22	.6655	.6653	.6646	.6635	.6621	.6606	.6590	.6576	.6565	.6557	.6555
.24	.7044	.7042	.7037	.7029	.7018	.7006	.6994	.6983	.6974	.6968	.6966
.26	.7436	.7434	.7430	.7424	.7415	.7406	.7396	.7588	.7381	.7377	.7375
.28	.7829	.7828	.7825	.7820	.7813	.7806	.7798	.7792	.7787	.7783	.7782
0.30	0.8224	0.8223	0.8221	0.8217	0.8211	0.8206	0.8200	0.8195	0.8191	0.8188	0.8187
.32	.8620	.8619	.8617	.8614	.8610	.8606	.8601	.8597	.8594	.8592	.8592
.34	.9017	.9016	.9015	.9012	.9009	.9006	.9002	.8999	.8997	.8995	.8995
.36	.9415	.9414	.9413	.9411	.9409	.9406	.9403	.9401	.9399	.9398	.9397
.38	.9813	.9812	.9811	.9810	.9808	.9806	.9804	.9802	.9800	.9800	.9799
0.40	1.0211	1.0211	1.0210	1.0209	1.0207	1.0206	1.0204	1.0203	1.0201	1.0201	1.0201
.42	1.0610	1.0610	1.0609	1.0608	1.0607	1.0606	1.0604	1.0603	1.0602	1.0602	1.0602
.44	1.1009	1.1009	1.1008	1.1008	1.1007	1.1006	1.1005	1.1004	1.1003	1.1003	1.1003
.46	1.1408	1.1408	1.1408	1.1407	1.1407	1.1406	1.1405	1.1404	1.1404	1.1403	1.1403
.48	1.1808	1.1807	1.1807	1.1807	1.1806	1.1806	1.1805	1.1805	1.1804	1.1804	1.1804
0.50	1.2207	1.2207	1.2207	1.2206	1.2206	1.2206	1.2205	1.2205	1.2204	1.2204	1.2204
.52	1.2607	1.2607	1.2607	1.2606	1.2606	1.2606	1.2605	1.2605	1.2605	1.2605	1.2605
.54	1.3007	1.3006	1.3006	1.3006	1.3006	1.3006	1.3005	1.3005	1.3005	1.3005	1.3005
.56	1.3406	1.3406	1.3406	1.3406	1.3406	1.3406	1.3405	1.3405	1.3405	1.3405	1.3405
.58	1.3806	1.3806	1.3806	1.3806	1.3806	1.3806	1.3805	1.3805	1.3805	1.3805	1.3805
0.60	1.4206	1.4206	1.4206	1.4206	1.4206	1.4206	1.4205	1.4205	1.4205	1.4205	1.4205
.62	1.4606	1.4606	1.4606	1.4606	1.4606	1.4606	1.4605	1.4605	1.4605	1.4605	1.4605
.64	1.5006	1.5006	1.5006	1.5006	1.5006	1.5006	1.5005	1.5005	1.5005	1.5005	1.5005
.66	1.5406	1.5406	1.5406	1.5406	1.5406	1.5406	1.5406	1.5405	1.5405	1.5405	1.5405
.68	1.5806	1.5806	1.5806	1.5806	1.5806	1.5806	1.5806	1.5805	1.5805	1.5805	1.5805
0.70	1.6206	1.6206	1.6206	1.6206	1.6206	1.6206	1.6206	1.6205	1.6205	1.6205	1.6205

TABLE I. COORDINATES OF $f_2(x-x_o,\ y-y_o)$—Concluded

(b) Values of $(x-x_o)/S$

f_2 ↓ \ $\frac{y-y_o}{S}$ →	0	0.025	0.050	0.075	0.100	0.125	0.150	0.175	0.200	0.225	0.250
−0.40	0.0258	0.0060									
−.38	.0293	.0151									
−.36	.0332	.0217									
−.34	.0377	.0281									
−.32	.0428	.0346									
−0.30	0.0485	0.0414									
−.28	.0551	.0489	0.0219								
−.26	.0625	.0572	.0367								
−.24	.0710	.0663	.0496								
−.22	.0808	.0766	.0625	0.0256							
−0.20	0.0918	0.0882	0.0761	0.0500							
−.18	.1046	.1013	.0908	.0700	0.0148						
−.16	.1192	.1163	.1071	.0897	.0571						
−.14	.1362	.1336	.1254	.1105	.0854	0.0317					
−.12	.1559	.1535	.1462	.1330	.1123	.0782					
−0.10	0.1791	0.1769	0.1702	0.1585	0.1405	0.1137	0.0685				
−.08	.2068	.2047	.1985	.1877	.1717	.1490	.1160	0.0572			
−.06	.2405	.2386	.2326	.2225	.2076	.1873	.1598	.1204	0.0463		
−.04	.2837	.2816	.2756	.2654	.2509	.2317	.2068	.1743	.1200	0.0408	
−.02	.3437	.3414	.3344	.3229	.3072	.2871	.2624	.2321	.1942	.1432	0.0487

U. S. GOVERNMENT PRINTING OFFICE: 1949

APPENDIX C

SYMBOLS

The principal symbols used throughout the report are listed here for convenience of reference.

$f_1 \equiv$ $\frac{1}{4\pi}\log\left[(x-x_o)^2+(y-y_o)^2\right]$

$f_2 \equiv$ $\frac{1}{4\pi}\log\left[\sin^2\frac{\pi}{S}(x-x_o)+\sinh^2\frac{\pi}{S}(y-y_o)\right]$

K natural logarithm of distance from singular point to center of circle corresponding to cascade airfoil

l total arc length of airfoil

S distance between successive airfoils in cascade

s arc-length parameter corresponding to z

s_o arc-length parameter corresponding to z_o

V magnitude of uniform or mean stream velocity in airfoil or cascade plane (fig. 1)

V_c magnitude of uniform stream velocity in circle plane

V_x x-component of uniform or mean stream velocity V

$V_{x,r}$ resultant local mean stream x-component of velocity V

V_y y-component of uniform or mean stream velocity V

v_c local velocity on circle corresponding to isolated airfoil

$v_{c,c}$ local velocity on circle corresponding to airfoil in cascade

v_x velocity induced by vortices in region $f_2>0$

w complex potential function, $\varphi+i\psi$

w_m' complex velocity of mean stream for airfoil in cascade

$$\left[w_m'=\frac{1}{2}(w_1'+w_2')=V_x-iV_y\right]$$

w_u' complex velocity of uniform stream for isolated airfoil, V_x-iV_y

x real part of z

x_c, y_c coordinates of point about which airfoil is rotated (centroid of vortex distribution for cascade airfoils)

y imaginary part of z

z coordinate of point where stream function is computed, $x+iy$

z_o coordinate of point where vortex is located, x_o+iy_o

α angle of inclination of uniform stream velocity to x-axis

β angle through which airfoil is rotated

Γ circulation about airfoil

$\gamma(z_o)$ vortex strength per unit arc length at z_o

θ central angle of circle

θ_N angle of stagnation point on circle corresponding to leading edge of airfoil

θ_T angle of stagnation point on circle corresponding to trailing edge of airfoil

λ angle of inclination of mean flow to normal to ca axis (fig. 1)

φ velocity potential on airfoil, $R[w(z)]$

$\varphi_A, \varphi_B,$ values of φ at points A, B, C, D, respectively,

φ_C, φ_D curve of $\varphi(s_o)$ intersects $f_2(s, s_o)=0$ (See fig.

φ_c velocity potential on circle corresponding to is airfoil

$\varphi_{c,c}$ velocity potential on circle corresponding to air cascade

φ_{min} velocity potential at leading edge of airfoil

ψ stream function, $I[w(z)]$

ψ_m stream function of mean stream of cascade flow

ψ_u stream function of uniform stream flowing isolated airfoil

$\overline{\psi}$ mean value of stream function over airfoil

$\Delta\psi$ variation of stream function, $\psi-\overline{\psi}$

Subscripts 1 and 2 when appended to w', V, and V_x in inflow and discharge values, respectively.

REFERENCES

1. Mutterperl, William: The Conformal Transformation of an U4765 into a Straight Line and Its Application to the Inverse Pr of Airfoil Theory. NACA ARR No. L4K22a, 1944.
2. Theodorsen, Theodore: Airfoil-Contour Modifications Bas ε-Curve Method of Calculating Pressure Distribution. ARR No. L4G05, 1944.
3. Mutterperl, William: A Solution of the Direct and Inverse tial Problems for Arbitrary Cascades of Airfoils. NACA No. L4K22b, 1944.
4. Ackeret, J.: The Design of Closely Spaced Blade Grids. R. T. P. Trans. No. 2007, Ministry Aircraft Prod. Schweiz. Bauzeitung, vol. 120, no. 9, Aug. 29, 1942, pp. 103
5. von Mises, Richard, and Friedrichs, Kurt O.: Fluid Dyn Advance Instruction and Research in Mechanics, ch. Brown Univ., Summer, 1941, pp. 96–97.
6. Stodola, A.: Steam and Gas Turbines, vol. II. McGraw Book Co., Inc., 1927, pp. 992–994. (Reprinted, Peter (New York), 1945.)
7. von Kármán, Th.: Compressibility Effects in Aerodyna Jour. Aero. Sci., vol. 8, no. 9, July 1941, pp. 337–356.
8. Garrick, I. E., and Kaplan, Carl: On the Flow of a Compre Fluid by the Hodograph Method. I—Unification and Exte of Present-Day Results. NACA Rep. No. 789, 1944.
9. Theodorsen, T., and Garrick, I. E.: General Potential Theo Arbitrary Wing Sections. NACA Rep. No. 452, 1933.
10. Garrick, I. E.: On the Plane Potential Flow past a Symme U1397 Lattice of Arbitrary Airfoils. NACA Rep. No. 788, 1944.
11. Gebelein, H : Theory of Two-Dimensional Potential Flow Arbitrary Wing Sections. NACA TN No. 886, 1939.

TABLE I. COORDINATES OF $f_2(x-x_o,\ y-y_o)$

(a) Values of $(y-y_o)/S$

f_2 ↓ \ $\frac{x-x_o}{S}$ →	0	0.05	0.10	0.15	0.20	0.25	0.30	0.35	0.40	0.45	0.50
−0.40	0.0257										
−.38	.0292										
−.36	.0331										
−.34	.0375										
−.32	.0425										
−0.30	0.0481										
−.28	.0545	0.0229									
−.26	.0618	.0371									
−.24	.0699	.0497									
−.22	.0791	.0621									
−0.20	0.0894	0.0750									
−.18	.1010	.0887	0.0296								
−.16	.1140	.1035	.0620								
−.14	.1286	.1195	.0871								
−.12	.1447	.1369	.1107	0.0392							
−0.10	0.1626	0.1560	0.1344	0.0881							
−.08	.1824	.1768	.1588	.1241	0.0454						
−.06	.2041	.1993	.1844	.1572	.1103						
−.04	.2277	.2236	.2113	.1896	.1558	0.1014					
−.02	.2532	.2198	.2396	.2222	.1966	.1608	0.1096				
0	0.2805	0.2778	0.2694	0.2553	0.2354	0.2096	0.1777	0.1400	0.0969	0.0496	0.0000
.02	.3097	.3074	.3006	.2892	.2737	.2542	.2318	.2081	.1858	.1692	.1629
.04	.3405	.3386	.3331	.3239	.3117	.2968	.2804	.2638	.2491	.2389	.2352
.06	.3728	.3713	.3668	.3595	.3498	.3384	.3260	.3139	.3036	.2965	.2940
.08	.4064	.4052	.4016	.3958	.3881	.3793	.3698	.3608	.3533	.3482	.3464
0.10	0.4412	0.4402	0.4373	0.4327	0.4267	0.4198	0.4126	0.4058	0.4001	0.3964	0.3951
.12	.4769	.4761	.4739	.4702	.4655	.4601	.4545	.4493	.4451	.4423	.4413
.14	.5135	.5129	.5111	.5082	.5045	.5003	.4960	.4920	.4888	.4867	.4859
.16	.5508	.5503	.5488	.5466	.5437	.5404	.5371	.5340	.5316	.5299	.5294
.18	.5886	.5882	.5871	.5853	.5830	.5805	.5779	.5735	.5736	.5724	.5720
0.20	0.6269	0.6266	0.6257	0.6243	0.6225	0.6205	0.6185	0.6167	0.6152	0.6143	0.6140
.22	.6655	.6653	.6646	.6635	.6621	.6606	.6590	.6576	.6565	.6557	.6555
.24	.7044	.7042	.7037	.7029	.7018	.7006	.6994	.6983	.6974	.6968	.6966
.26	.7436	.7434	.7430	.7424	.7415	.7406	.7396	.7588	.7381	.7377	.7375
.28	.7829	.7828	.7825	.7820	.7813	.7806	.7798	.7792	.7787	.7783	.7782
0.30	0.8224	0.8223	0.8221	0.8217	0.8211	0.8206	0.8200	0.8195	0.8191	0.8188	0.8187
.32	.8620	.8619	.8617	.8614	.8610	.8606	.8601	.8597	.8594	.8592	.8592
.34	.9017	.9016	.9015	.9012	.9009	.9006	.9002	.8999	.8997	.8995	.8995
.36	.9415	.9414	.9413	.9411	.9409	.9406	.9403	.9401	.9399	.9398	.9397
.38	.9813	.9812	.9811	.9810	.9808	.9806	.9804	.9802	.9800	.9800	.9799
0.40	1.0211	1.0211	1.0210	1.0209	1.0207	1.0206	1.0204	1.0203	1.0201	1.0201	1.0201
.42	1.0610	1.0610	1.0609	1.0608	1.0607	1.0606	1.0604	1.0603	1.0602	1.0602	1.0602
.44	1.1009	1.1009	1.1008	1.1008	1.1007	1.1006	1.1005	1.1004	1.1003	1.1003	1.1003
.46	1.1408	1.1408	1.1408	1.1407	1.1407	1.1406	1.1405	1.1404	1.1404	1.1403	1.1403
.48	1.1808	1.1807	1.1807	1.1807	1.1806	1.1806	1.1805	1.1805	1.1804	1.1804	1.1804
0.50	1.2207	1.2207	1.2207	1.2206	1.2206	1.2206	1.2205	1.2205	1.2204	1.2204	1.2204
.52	1.2607	1.2607	1.2607	1.2606	1.2606	1.2606	1.2605	1.2605	1.2605	1.2605	1.2605
.54	1.3007	1.3006	1.3006	1.3006	1.3006	1.3006	1.3005	1.3005	1.3005	1.3005	1.3005
.56	1.3406	1.3406	1.3406	1.3406	1.3406	1.3406	1.3405	1.3405	1.3405	1.3405	1.3405
.58	1.3806	1.3806	1.3806	1.3806	1.3806	1.3806	1.3805	1.3805	1.3805	1.3805	1.3805
0.60	1.4206	1.4206	1.4206	1.4206	1.4206	1.4206	1.4205	1.4205	1.4205	1.4205	1.4205
.62	1.4606	1.4606	1.4606	1.4606	1.4606	1.4606	1.4605	1.4605	1.4605	1.4605	1.4605
.64	1.5006	1.5006	1.5006	1.5006	1.5006	1.5006	1.5005	1.5005	1.5005	1.5005	1.5005
.66	1.5406	1.5406	1.5406	1.5406	1.5406	1.5406	1.5406	1.5405	1.5405	1.5405	1.5405
.68	1.5806	1.5806	1.5806	1.5806	1.5806	1.5806	1.5806	1.5805	1.5805	1.5805	1.5805
0.70	1.6206	1.6206	1.6206	1.6206	1.6206	1.6206	1.6206	1.6205	1.6205	1.6205	1.6205

TABLE I. COORDINATES OF $f_2(x-x_o,\ y-y_o)$—Concluded

(b) Values of $(x-x_o)/S$

f_2 ↓ \ $\frac{y-y_o}{S}$ →	0	0.025	0.050	0.075	0.100	0.125	0.150	0.175	0.200	0.225	0.250
−0.40	0.0258	0.0060									
−.38	.0293	.0151									
−.36	.0332	.0217									
−.34	.0377	.0281									
−.32	.0428	.0346									
−0.30	0.0485	0.0414									
−.28	.0551	.0489	0.0219								
−.26	.0625	.0572	.0367								
−.24	.0710	.0663	.0496								
−.22	.0808	.0766	.0625	0.0256							
−0.20	0.0918	0.0882	0.0761	0.0500							
−.18	.1046	.1013	.0908	.0700	0.0148						
−.16	.1192	.1163	.1071	.0897	.0571						
−.14	.1362	.1336	.1254	.1105	.0854	0.0317					
−.12	.1559	.1535	.1462	.1330	.1123	.0782					
−0.10	0.1791	0.1769	0.1702	0.1585	0.1405	0.1137	0.0685				
−.08	.2068	.2047	.1985	.1877	.1717	.1490	.1160	0.0572			
−.06	.2405	.2386	.2326	.2225	.2076	.1873	.1598	.1204	0.0463		
−.04	.2837	.2816	.2756	.2654	.2509	.2317	.2068	.1743	.1290	0.0408	
−.02	.3437	.3414	.3344	.3229	.3072	.2871	.2624	.2321	.1942	.1432	0.0487

U. S. GOVERNMENT PRINTING OFFICE: 1949

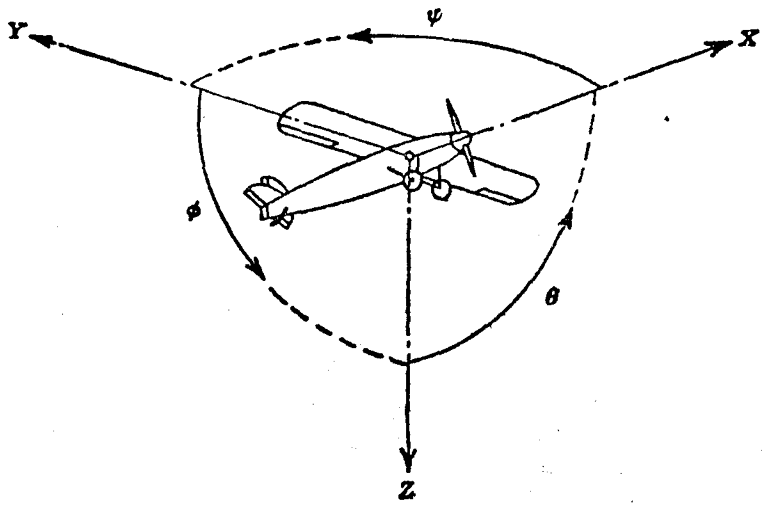

Positive directions of axes and angles (forces and moments) are shown by arrows

Axis		Force (parallel to axis) symbol	Moment about axis			Angle		Velocities	
Designation	Symbol		Designation	Symbol	Positive direction	Designation	Symbol	Linear (component along axis)	Angular
Longitudinal	X	X	Rolling	L	$Y \longrightarrow Z$	Roll	ϕ	u	p
Lateral	Y	Y	Pitching	M	$Z \longrightarrow X$	Pitch	θ	v	q
Normal	Z	Z	Yawing	N	$X \longrightarrow Y$	Yaw	ψ	w	r

Absolute coefficients of moment

$C_l=\frac{L}{qbS}$ (rolling) $C_m=\frac{M}{qcS}$ (pitching) $C_n=\frac{N}{qbS}$ (yawing)

Angle of set of control surface (relative to neutral position), δ. (Indicate surface by proper subscript.)

4. PROPELLER SYMBOLS

D Diameter

p Geometric pitch

p/D Pitch ratio

V' Inflow velocity

V_s Slipstream velocity

T Thrust, absolute coefficient $C_T=\frac{T}{\rho n^2 D^4}$

Q Torque, absolute coefficient $C_Q=\frac{Q}{\rho n^2 D^5}$

P Power, absolute coefficient $C_P=\frac{P}{\rho n^3 D^5}$

C_s Speed-power coefficient $=\sqrt[5]{\frac{\rho V^5}{P n^2}}$

η Efficiency

n Revolutions per second, rps

Φ Effective helix angle $=\tan^{-1}\left(\frac{V}{2\pi rn}\right)$

5. NUMERICAL RELATIONS

1 hp=76.04 kg-m/s=550 ft-lb/sec

1 metric horsepower=0.9863 hp

1 mph=0.4470 mps

1 mps=2.2369 mph

1 lb=0.4536 kg

1 kg=2.2046 lb

1 mi=1,609.35 m=5,280 ft

1 m=3.2808 ft

ATI-71 140

National Advisory Committee for Aeronautics, Lewis Flight Propulsion Lab., Cleveland, O. (869)
ISOLATED AND CASCADE AIRFOILS WITH PRESCRIBED VELOCITY DISTRIBUTION - AND APPENDIXES A-C, by Arthur W. Goldstein and Meyer Jerison. 1947. 19 pp. UNCLASSIFIED

(Not abstracted)

DIVISION: Aerodynamics (2)
SECTION: Wings and Airfoils (6)
DISTRIBUTION: U. S. Military Organizations request copies from ASTIA-DSC. Others route requests to ASTIA-DSC thru AMC, Wright-Patterson Air Force Base, Dayton, O. Attn: NACA.

I. Goldstein, Arthur W.
II. Jerison, Meyer